TECHNICAL MEMORANDUMS

NATIONAL ADVISORY COMMITTEE FOR AERONAUTICS

No. 835

PRESSURE DISTRIBUTION ON A WING SECTION WITH

SLOTTED FLAP IN FREE FLIGHT TESTS

By Georg Kiel

NATIONAL ADVISORY COMMITTEE FOR AERONAUTICS

TECHNICAL MEMORANDUM NO. 835

PRESSURE DISTRIBUTION ON A WING SECTION WITH

SLOTTED FLAP IN FREE FLIGHT TESTS*

By Georg Kiel

The pressure distribution was measured in flight on a wing section with a slotted flap for several flap deflections, and the results obtained are here presented. The test apparatus and the procedure employed in obtaining the results are also described. A Fieseler type F 5 R airplane was used for the tests.

INTRODUCTION

No flight test results on pressure-distribution measurements on wing sections with flaps have heretofore been available. Reliable data on the magnitude of the actual aerodynamic forces set up in flight and the manner in which they are set up are of great importance, however, to the practicing designer. Such data may be obtained only by flight tests and therefore pressure-distribution tests were conducted in free flight at various flap settings.

Since the results are similar for wing sections extending over the region of the ailerons the measurements may, in particular cases, also provide data on the pressure distribution at the ailerons, a result which is of particular importance in view of the fact that a whole series of aileron failures in recent years has indicated that the actual stresses arising in flight may so far exceed those computed from theory that crack-ups and damage to the airplane may result.

Since no pressure-distribution tests in flight have as yet been carried out in Germany and no experimental data have been available these measurements provide at the

---

same time a means for determining and checking a suitable test procedure.

AIRPLANE TESTED AND INSTRUMENTS INSTALLED

For the purposes of these tests, an airplane of type Fieseler F 5 R was employed. Figure 1 shows the test airplane with deflected flap in flight. For the pressure-distribution measurements, a wing section was chosen that lay outside the propeller slipstream. Figure 2 shows a sketch of the airplane and the section investigated. Figure 3 shows how the pressures at the wing surface were taken. Great care was taken to see that the pressure tubes were set flush with the surface. In order to avoid even very slight unevenness the wing surface, where the orifices were drilled, was ground smooth and lacquered over again. Figure 4 shows the pressure orifices on the upper surface, and figure 5 the pressure orifices on the upper side of the flap, the latter being shown fully deflected. With the flap neutral, the slot seen in figure 5 is closed and the two forward measuring orifices on the upper surface of the flap then disappear into the closed slot, so that with the flap neutral they are not employed. From the orifices aluminum tubes arranged in the wing interior lead to measuring apparatus in the fuselages. For recording the pressures at each station, four optical DVL double-recording manometers were employed. Two of these were located in the cockpit and two in the baggage compartment, figures 6 and 7 showing the manner of installation. At the cockpit there was in addition an optical dynamic pressure-recording manometer for recording the dynamic pressures in flight and a storage battery for feeding the lamps and motors in the recording apparatus. Furthermore, a Wetzer-type clock mechanism was installed at the same place that marked off short time intervals during the tests, thus providing an accurate time scale for the records of the several recording instruments. The entire pressure-measuring apparatus could be simultaneously connected in by the pilot through a common main switch (fig. 8). The clockwork was set in motion for the interval during which the tests were conducted by means of a rod arrangement leading to the observer.

TEST PROCEDURE

The test procedure consisted in taking the pressure at each station by means of the optical manometers described above at various dynamic pressures with the airplane in level unaccelerated flight.

To determine the undisturbed dynamic pressure in flight, the Prandtl tube shown in the photograph (fig. 9) was calibrated for the several flap settings. The total pressure was obtained by a total pressure apparatus located at the under surface of the wing (fig. 9) and the static pressure by a towed static tube towed in the undisturbed stream below the airplane (reference 1); figure 10 shows the static tube at the fuselage in the drawn-in position. The calibration curves for each of the flap settings are given in figure 11, the readings being plotted against the actual dynamic pressures in flight.

The double recording manometers for measuring the pressure distribution were statically calibrated by means of a fluid manometer, figure 12 showing one such calibration curve. The apparatus, which was employed in these measurements for the first time to any large extent, proved to be reliable. It is worth noting that the pressure tubes showed practically no hysteresis of any kind. Figure 13 shows an example of a dynamic pressure record obtained in flight and the pressure record of a recording manometer.* Figure 14 shows the wing profile at the test section with the position of the orifices measured from the leading edge of the wing parallel to the reference line shown in the figure. The pressure orifices at the upper and lower surfaces of the wing were arranged one above the other at right angles to the reference line. Altogether there were 24 orifices distributed over the entire wing section. Since, however, only four double manometers - that is, altogether eight manometers were available, each pair of orifices was connected to one manometer as shown on figure 15, and thus the sum of the pressures on the upper and

---

*On the basis of the favorable results obtained with the optical double manometer of the DVL, a 40-fold recording manometer was developed at the Institute for Flight Mechanics of the DVL that works on the same principle and which may be applied to pressure-distribution measurements for unaccelerated as well as for accelerated flight conditions.

under side of the wing was approximately measured. The
advantage of this method of measuring lay in the fact that
with the measuring apparatus available, twice as many or-
ifices could be utilized as there were manometers. The
pressures at 16 orifices could thus be simultaneously re-
corded. This number of orifices would be too few, how-
ever, to give an accurate determination of the pressure
distribution, particularly when the flap was deflected.
It was thus not possible to measure simultaneously during
a single flight the pressures at the total number of posi-
tions required. Only some of the orifices were therefore
utilized in one flight and then the remainder in a second
flight. In order to obtain the same conditions for all
flight tests the take-off weight was always kept the same.
The mean weight of the airplane (between take-off and land-
ing) was 585 kilograms, and the mean wing loading was
$G/F = 42.5$ kg/m^2 (8.70 lb./sq.ft.).

RESULTS AND DISCUSSION OF THE FLIGHT-TEST MEASUREMENTS

To draw the pressure-distribution curves it was nec-
essary to have the simultaneous pressures at all the
points at equal dynamic pressure. On account of the prac-
tical difficulty described above, of obtaining all the
pressures simultaneously at the same dynamic pressure, the
ratio p/q of the pressure, measured at some definite
point, to the dynamic pressure was plotted against the dy-
namic pressure. Figure 16, (a) and (b), shows the pres-
sure at each of the test positions as a function of the
dynamic pressure with flap neutral; figure 17, (a) to (c),
for the flap deflected 19°, and figure 18, (a) to (e), for
the flap deflected 32°. This method has the advantage
that good mean values are obtained at each flight condi-
tion for each of the measuring stations and accidental
values of a single measurement eliminated.

In order to present values that are generally valid
the pressure distribution will be given for different lift
coefficients of the airplane. Since the measurements were
conducted in straight level flight, the lift may be set
equal to the weight $(A = G)$. The lift coefficient for
the complete airplane will then be $c_{a_{total}}{}^* = G/F_q$. For
each value of the dynamic pressure corresponding to the
same $c_{a_{total}}$ the p/q values for each of the measuring
positions were read off from the $p/q = f(q)$ curves.

---

*$c_{a_{ges}} = c_{a_{total}}$

With these values the pressure-distribution curve over the wing chord was drawn. Figure 19, (a) to (i), shows the pressure distribution for zero flap deflection; figure 20, (a) to (k), for a flap deflection of 19°; and figure 21, (a) to (k), for a deflection of 32°. The points indicated are not values obtained directly by measurement but mean values taken from the $p/q = f(q)$ curves.

With the flap neutral and at small values of $c_{a_{total}}$ and c_n the pressure-distribution curves have a more rounded form. With increasing values of c_n the pressure in the neighborhood of the airfoil leading edge increases rapidly.

With a flap deflection of 19° the pressure-distribution curves show a somewhat fuller or more rounded form. For equal normal force coefficient the pressure at the wing nose is less than with the flap neutral. Of particular interest is the rather steep pressure rise near the leading edge of the flap. In the region of the flap the pressure-distribution curve assumes a shape similar to that for a wing alone. At a flap deflection of 19° there is relatively only a small change, over the total normal flight range, in the maximum values of p/q at the nose of the flap as well as in the entire pressure distribution over the flap. Evidently the flow is so directed by the main wing that the flap experiences only a slight change in the wind direction.

With a flap deflection of 32° there is a marked increase in the pressure at the leading edge of the flap, the pressure, at small values of c_n considerably exceeding that at the leading edge of the wing, as may be seen from figure 21, (a) to (c). With increasing values of c_n a rather steep peak is built up at the wing nose while the p/q value at the flap leading edge increases at an appreciably lower rate.

Tables I to III give the mean values for all the measurements. On these tables and also on the individual pressure-distribution curves there are also indicated the normal force coefficients of the wing section investigated, as well as the moment coefficients c_m with respect to the leading edge of the wing and wing chord of the section investigated. The normal force coefficient may, with sufficiently good approximation, be obtained by integrating the pressure distribution over the wing chord. With the

notation of figure 22, the normal force coefficient of the
wing section is

$$c_n = \frac{1}{t} \int_o^t \frac{p}{q} \, dx$$

The normal force coefficient over the wing section is thus
simply obtained by planimetering the pressure distribution
curves and dividing by the wing chord   t.   The normal
force coefficient with the flap deflected was based on the
same wing chord as with the flap neutral.   (See fig. 22.)
With the flap deflected we may write for the normal force
coefficient

$$c_n = \frac{1}{t} \left(\int_o^{x_1} \frac{p}{q} \, dx + \cos \beta \int_{x_1}^t \frac{p}{q} \, dx \right)$$

Figure 23 shows the normal force coefficients thus obtained
for each deflection as a function of the lift coefficient
$c_{a_{total}}$ for the complete airplane, and figure 24 shows
the normal force coefficient for the flap alone c_{nk} as a
function of the lift coefficient $c_{a_{total}}$ for the com-
plete airplane, the normal force being at right angles to
the flap chord.   (See sketch at upper right-hand corner of
fig. 24.)   With this definition, the normal force coeffi-
cient of the flap is

$$c_{nk} = \frac{1}{t_k} \int_o^{t_k} \frac{p}{q} \, dx$$

In a similar manner the moment coefficient may be ob-
tained.   The moment coefficient of the wing section is

$$c_m = \frac{1}{t^2} \int_o^t \frac{p}{q} \, x \, dx$$

In the region of the flap we must again multiply by the
cosine of the flap deflection angle so that for the de-
flected flap (see fig. 22) the moment coefficient is

$$c_m = \frac{1}{t^2} \left(\int_0^{x_1} \frac{p}{q} \, x \, dx + \cos \beta \int_{x_1}^{t} \frac{p}{q} \, x \, dx \right)$$

Figure 25 shows the moment coefficient c_m of the investigated wing section as a function of the normal force coefficient c_n for the several flap deflections ($\beta = 0^\circ$, 19°, 32°). The curves $c_m = f(c_n)$ for all flap deflections have the usual normal appearance. With increasing flap deflection the moment coefficient increases rapidly. From the slope of the curves of figure 25 the partial differential coefficient $\frac{\partial c_m}{\partial c_n}$, which always has a constant value in the normal range of angles of attack, may be read off.

For a flap deflection of 0° and 19° the value $\frac{\partial c_m}{\partial c_n} = 0.247$ is obtained; for $\beta = 32^\circ$ the value obtained is $\frac{\partial c_m}{\partial c_n} = 0.252$. A good agreement is everywhere obtained between this value and the result of the hydrodynamic theory for wing sections according to which for all profiles $\frac{\partial c_m}{\partial c_n} = 0.25$.*

Figure 26 shows, finally, the effect of the flap deflection on the pitching moment at zero lift, the moment coefficients c_{m_0} being plotted against the flap deflection for $c_n = 0$. The c_{m_0} values are obtained for the different flap deflections by extrapolation from the curves $c_m = f(c_n)$ of figure 25. In the normal flight range, as is well known, a linear relation holds, for all profiles, between the moment coefficient, the normal force coefficient, and the flap deflection. The moment coefficient is

$$c_m = \overline{c_{m_0}} + \frac{\partial c_m}{\partial \beta} \, \beta + \frac{\partial c_m}{\partial c_n} \, c_n$$

where $\overline{c_{m_0}}$ denotes the moment coefficient for zero flap deflection corresponding to $c_n = 0$. In our case $\overline{c_{m_0}} = 0.015$. From figure 26 the value obtained for $\frac{\partial c_m}{\partial \beta}$ is

----

*In the given case c_n may be set equal to c_a.

0.0068. By substituting the values found for $\dfrac{\partial c_m}{\partial \beta}$ and

$\dfrac{\partial c_m}{\partial c_n}$ the moment coefficient for the section under investi-

gation is found to be

$$c_m = 0.015 + 0.0068 \ \beta + 0.25 \ c_n$$

For completeness there is shown on figure 27 the cen-
ter of pressure travel for the several flap deflections
as a function of the normal force coefficient c_n. With
the flap neutral the position of the center of pressure,
within the normal flight range, varies only slightly.
With the flap deflected 19° and 32° the center of pressure
moves backward a relatively large amount, the position of
the center of pressure showing a greater dependence on c_n.
With decreasing values of c_n, that is, with increasing
velocity, the center of pressure, for relatively large val-
ues of c_n travels backward a considerable amount.

<center>SUMMARY</center>

Pressure-distribution curves were obtained in unaccel-
erated flight on a wing section with slotted flap at flap
deflections of 0°, 19°, 32°. The flap chord was 0.296
times the over-all wing chord. With a flap deflection of
19° the pressure-distribution curves show a somewhat fuller
form (that is, less peaked) than is the case with flap neu-
tral. For equal normal force coefficient the pressure in
the region of the nose of the wing is less than for zero
flap deflection. In the neighborhood of the flap leading
edge, with the flap deflected, a rather steep pressure
rise occurs, the pressure-distribution curve in this case
assuming a form similar to that of the wing alone. With
the flap deflected 19° there is only a relatively slight
change both in the maximum pressure at the flap leading
edge as well as in the general pressure distribution over
the flap. Evidently the main wing diverts the flow in
such a manner that the air-flow direction at the flap ex-
periences only a slight change. With a flap deflection of
32° a marked pressure rise occurs at the leading edge of
the flap, considerably exceeding that at the wing leading
edge at small normal force coefficients. As the normal
force coefficient increases a rather steep pressure peak
is built up at the nose of the wing while at the flap
leading edge the pressure increases at a considerably lower
rate.

By integrating the pressure-distribution curves the normal force and moment coefficients were determined. The effect of the flap deflection on the magnitude of the pitching moment at zero lift was also determined, agreement being found with hydrodynamic theory for $\dfrac{\partial c_m}{\partial c_n} = 0.25$. The value of $\dfrac{\partial c_m}{\partial \beta}$ was obtained as 0.0068.

If, for the moment coefficient, we set

$$c_m = \overline{c_{m_0}} + \frac{\partial c_m}{\partial \beta} \beta + \frac{\partial c_m}{\partial c_n} c_n$$

we obtain in our case

$$c_m = 0.015 + 0.0068 \, \beta + 0.25 \, c_n$$

For completeness, there is finally given the center of pressure travel as a function of the normal force coefficient.

In particular cases the results presented here may also provide information on the pressure distribution on ailerons insofar as the form of the latter corresponds to the flap arrangement discussed in this paper.

Translation by S. Reiss,
National Advisory Committee
for Aeronautics.

REFERENCE

1. Kiel, G.: Total-Head Meter with Small Sensitivity to Yaw. T.M. No. 775, N.A.C.A., 1935.

TABLE I.　Test Results for a Flap Deflection of　β = 0°

Total lift coefficient	$c_{a\,ges\,(total)}$	0,30	0,45	0,60	0,70	0,80	0,96	1,10	1,22	1,27
Normal force coefficient	c_n	0,36	0,51	0,65	0,77	0,87	1,03	1,16	1,27	1,33
Moment coefficient	c_m	0,11	0,14	0,18	0,21	0,23	0,27	0,30	0,31	0,33
Measuring station No.	Distance from wing leading edge percent, t					p/q				
1	2,5	0,34	0,99	1,58	2,00	2,35	2,92	3,39	3,88	4,22
2	5,0	0,61	1,14	1,63	1,97	2,29	2,80	3,27	3,65	3,88
3	10,0	0,74	1,12	1,51	1,78	2,05	2,48	2,85	3,17	3,33
4	20,0	0,81	1,05	1,33	1,52	1,71	2,01	2,26	2,48	2,59
5	30,0	0,64	0,80	1,00	1,12	1,24	1,43	1,60	1,74	1,80
6	40,0	0,51	0,64	0,78	0,88	0,96	1,09	1,18	1,27	1,29
7	50,0	0,36	0,44	0,54	0,61	0,68	0,76	0,82	0,88	0,90
8	60,0	0,23	0,29	0,36	0,40	0,45	0,50	0,55	0,58	0,59
11	81,4	0,04	0,05	0,08	0,10	0,12	0,14	0,17	0,19	0,19
12	90,0	0,04	0,04	0,07	0,08	0,09	0,11	0,12	0,12	0,12

TABLE II.　Test Results for a Flap Deflection of　β = 19°

Total lift coefficient	$c_{a\,ges\,(total)}$	0,45	0,60	0,70	0,80	1,00	1,20	1,40	1,44	1,52	1,67	1,77
Normal force coefficient	c_n	0,64	0,80	0,91	1,02	1,22	1,42	1,61	1,66	1,72	1,85	1,94
Moment coefficient	c_m	0,31	0,36	0,38	0,41	0,46	0,51	0,56	0,56	0,57	0,58	0,60
Measuring station No.	Distance from wing leading edge percent, t						p/q					
1	2,5	0,07	0,80	1,23	1,61	2,29	2,97	3,70	3,98	4,33	5,00	5,56
2	5,0	0,42	0,97	1,30	1,61	2,20	2,84	3,46	3,69	3,94	4,44	4,78
3	10,0	0,68	1,07	1,35	1,60	2,09	2,62	3,16	3,29	3,48	3,84	4,11
4	20,0	0,91	1,15	1,35	1,53	1,88	2,24	2,60	2,69	2,82	3,04	3,23
5	30,0	0,79	0,98	1,11	1,23	1,44	1,67	1,90	1,94	2,01	2,17	2,32
6	40,0	0,74	0,87	0,96	1,06	1,25	1,42	1,59	1,61	1,66	1,74	1,79
7	50,0	0,69	0,77	0,84	0,91	1,04	1,17	1,31	1,32	1,35	1,41	1,44
8	60,0	0,60	0,67	0,72	0,77	0,88	0,99	1,09	1,09	1,11	1,15	1,16
9	73,1	0,68	0,71	0,73	0,75	0,79	0,83	0,87	0,86	0,87	0,89	0,89
10	76,1	1,13	1,24	1,30	1,35	1,44	1,51	1,56	1,53	1,53	1,52	1,49
11	81,4	0,91	0,95	0,97	1,00	1,05	1,11	1,15	1,14	1,14	1,14	1,12
12	90,0	0,46	0,48	0,49	0,49	0,50	0,50	0,51	0,50	0,48	0,47	0,46

TABLE III.　Test Results for a Flap Deflection of　β = 32°

Total lift coefficient	$c_{a\,ges\,(total)}$	0,70	0,80	1,00	1,20	1,40	1,50	1,60	1,75	1,93	2,10	2,24
Normal force coefficient	c_n	0,97	1,10	1,32	1,54	1,73	1,84	1,93	2,07	2,23	2,44	2,56
Moment coefficient	c_m	0,48	0,51	0,56	0,63	0,67	0,70	0,72	0,75	0,79	0,86	0,87
Measuring station No.	Distance from wing leading edge percent, t						p/q					
1	2,5	0,51	1,01	1,86	2,72	3,46	3,84	4,15	4,67	5,35	6,22	6,87
2	5,0	0,93	1,23	1,85	2,52	3,16	3,47	3,77	4,22	4,74	5,39	5,96
3	10,0	0,98	1,34	1,90	2,41	2,88	3,13	3,36	3,74	4,20	4,69	5,05
4	20,0	1,21	1,45	1,82	2,16	2,52	2,71	2,87	3,12	3,40	3,69	3,92
5	30,0	1,06	1,20	1,45	1,69	1,94	2,06	2,16	2,31	2,49	2,68	2,84
6	40,0	1,02	1,12	1,31	1,48	1,66	1,74	1,81	1,90	2,03	2,14	2,24
7	50,0	1,00	1,07	1,20	1,33	1,47	1,54	1,60	1,66	1,78	1,87	1,94
8	60,0	0,95	0,99	1,08	1,18	1,28	1,33	1,38	1,44	1,52	1,59	1,64
9	73,1	1,89	1,93	2,03	2,13	2,24	2,29	2,33	2,37	2,47	2,56	2,66
10	76,1	2,50	2,54	2,64	2,74	2,85	2,91	2,96	2,98	3,08	3,15	3,20
11	81,4	1,35	1,35	1,39	1,45	1,52	1,55	1,58	1,60	1,66	1,71	1,74
12	90,0	0,64	0,66	0,71	0,73	0,75	0,76	0,76	0,75	0,76	0,75	0,74

Figure 1.- Test airplane with deflected flaps.

Leading edge

Pressure orifices covered when flap is undeflected
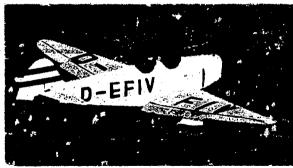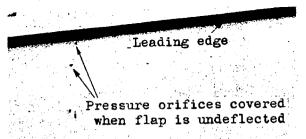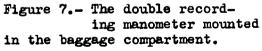
Figure 5.- Orifices on upper surface of flap. The picture shows the flap fully deflected (32°). With the flap neutral the slit seen on the picture is closed. The two orifices at the leading edge of the flap are then covered and in this case are not employed for pressure measurements.
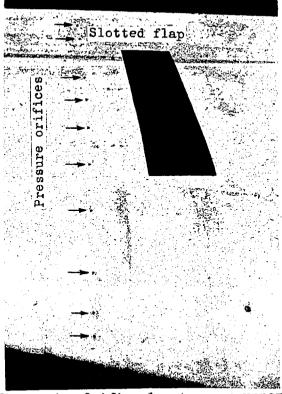
Slotted flap

Pressure orifices

Figure 4.- Orifice location on upper wing surface.

Optical dynamic pressure recorder

Wetzer contact mechanism

Pressure recorder
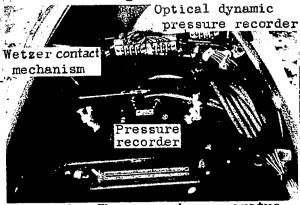
Figure 6.- The measuring apparatus installed in the cockpit.

Figure 7.- The double record-ing manometer mounted in the baggage compartment.

Wing covering (plywood)

Wooden block

Brass sheet

Brass pipe

Pressure lead to fuselage

Hose connection

Figure 3.- Installation of pressure tube in wing.

Wing section investigated
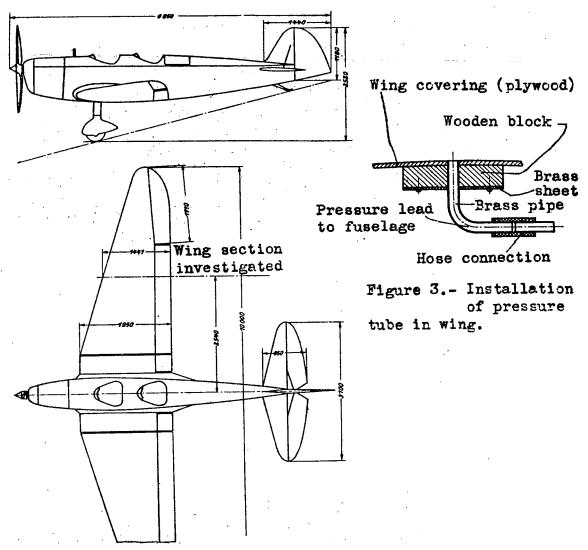
Figure 2.- Sketch of test airplane.

Height of pressure record

Flap deflection β - 0°

β - 79°

β - 38°
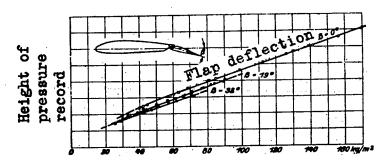
Figure 11.- Dynamic pressure calibration curves for the several flap deflections investigated.

Master
switch
Distributor
box
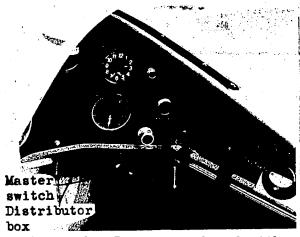
Figure 8.- Instrument board with
switch for connecting
in the measuring apparatus.
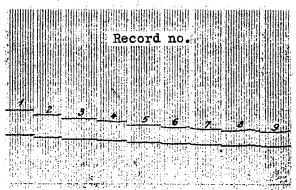
Record no.

Record no.

Figure 13.- Dynamic pressure record
obtained in flight and
corresponding pressure record of a
double recording manometer.
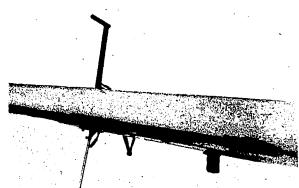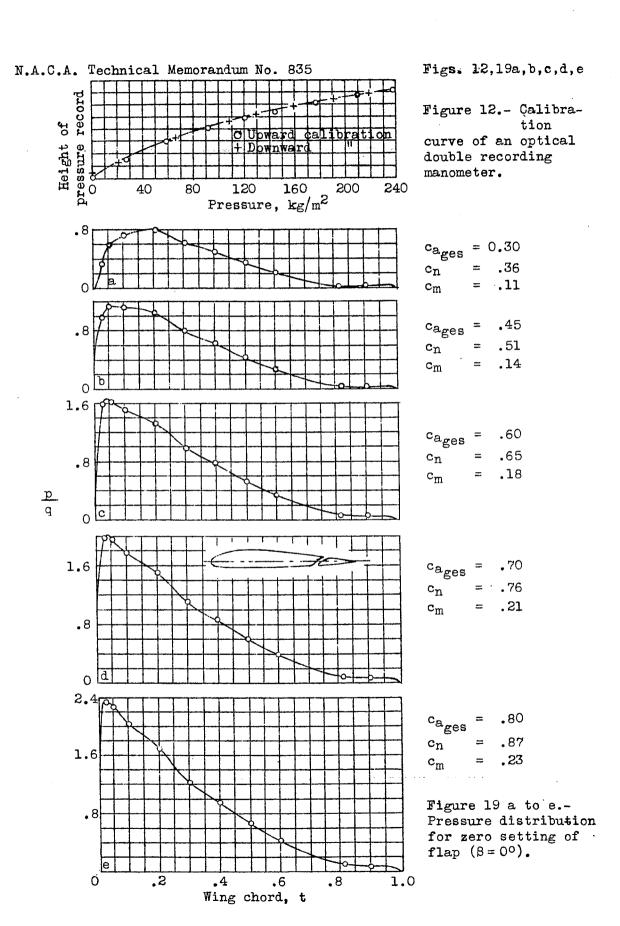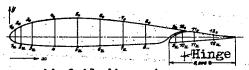
Figure 9.- Mounting of Prandtl tube
on the upper wing surface
for measuring the dynamic pressure
and of the total-pressure apparatus
at the lower wing surface.

Figure 10.- Suspension of static
pressure tube below
the fuselage (tube in drawn in
position).

Figure 12.- Calibra-
tion
curve of an optical
double recording
manometer.

$c_{a_{ges}}$ = 0.30
c_n = .36
c_m = .11

$c_{a_{ges}}$ = .45
c_n = .51
c_m = .14

$c_{a_{ges}}$ = .60
c_n = .65
c_m = .18

$c_{a_{ges}}$ = .70
c_n = .76
c_m = .21

$c_{a_{ges}}$ = .80
c_n = .87
c_m = .23

Figure 19 a to e.-
Pressure distribution
for zero setting of
flap ($\beta = 0°$).

Airfoil dimensions

x	0	1,25	2,5	5	7,5	10	15	20	30	40	50	60	70	80	90	95	100
y_o	0	2,75	3,78	4,57	5,60	6,40	7,50	8,22	8,85	8,90	7,27	6,08	4,18	2,80	1,03	0,46	0
y_u	0	-2,50	-3,18	-3,10	-3,50	-3,70	-4,00	-4,10	-4,32	-3,94	-3,43	-2,83	-2,51	-2,25	-1,86	-0,87	0

Arrangement of pressure orifices

Test sta.	1	2	3	4	5	6	7	8	9	10	11	12
Distance from L.E.,% of t	2,3	5,0	10,0	20,0	30,0	40,0	50,0	60,0	73,1	75,1	81,4	90,0

Figure 14.- Profile of section tested
with location of pressure
orifices.
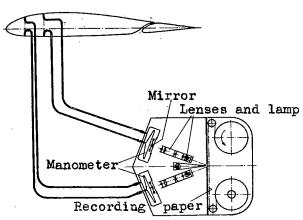
Figure 15.- Mounting of test apparatus
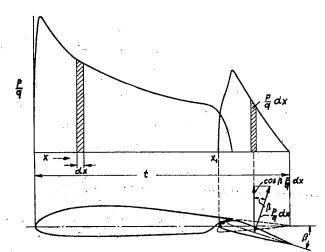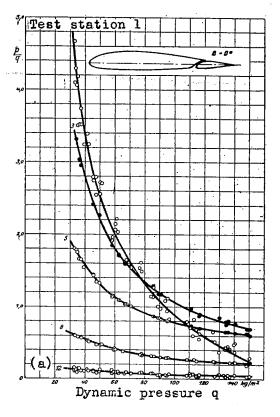
Figure 22.- Sketch to illustrate the
determination of the nor-
mal force and moment coefficients.
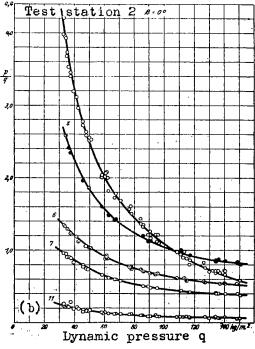
Figure 16(a,b.)- p/q as a function
of the dynamic pres-
sure q for zero flap deflection.

Test station 1

$\frac{p}{q}$

(a)

Dynamic pressure q

Test station 2

(b)

Dynamic pressure q

Test station 3

$\frac{p}{q}$

$\beta = 19°$

$\frac{p}{q}$

(c)

Dynamic pressure q

**Figure 17 (a) to (c).- p/q as a function of the dynamic
pressure q for a flap deflection, $\beta = 19°$**

Normal force coefficient
of flap, c_{nk}

$c_{nk} = \frac{1}{t_k} \int_0^{t_k} \frac{p}{q} \, dx$

$\beta = 32°$

$\beta = 19°$

Lift coefficient of the
complete airplane $c_{a_{ges}}$.
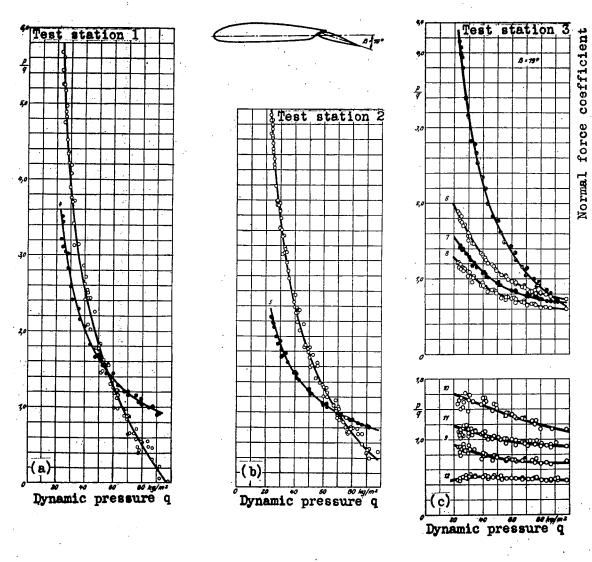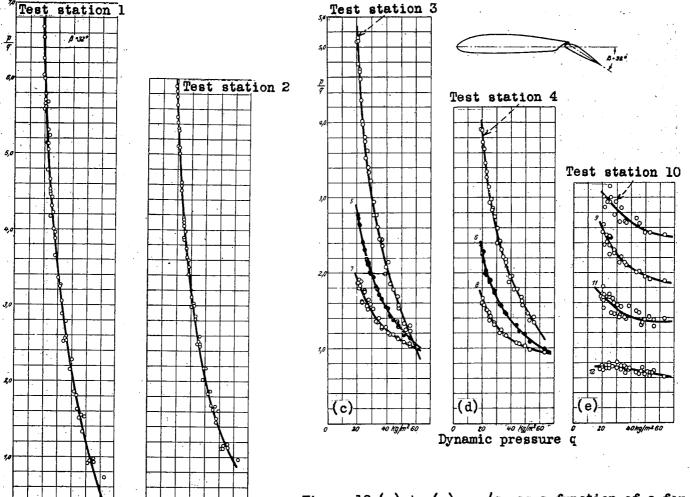
Figure 24.- Normal force
coefficient
c_{nk} of the flap alone as
a function of the lift
coefficient of the complete
airplane $c_{a_{ges}}$ for flap
deflections, $\beta = 19°$ and $32°$.

Test station 1

Test station 2

Test station 3

Test station 4

Test station 10

(a)

(b)

(c)

(d)

(e)

Dynamic pressure q

Dynamic pressure q

Figure 18 (a) to (e).- p/q as a function of q for a
flap deflection β = 32°

$c_{a_{ges}}$=0.96
c_n =1.03
c_m = .27

$c_{a_{ges}}$=1.10
c_n =1.16
c_m = .30

$c_{a_{ges}}$=1.22
c_n =1.27
c_m = .31
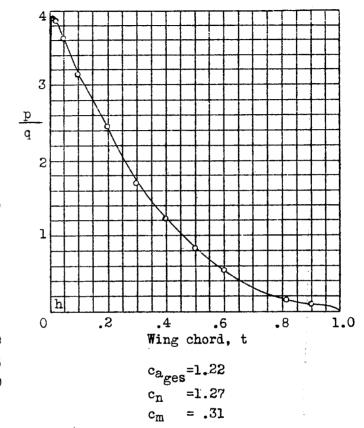
Figure 19f to h.- Pressure distribution for zero
setting of flap ($\beta = 0^{o}$).

$c_{a_{ges}} = 0.45$

$c_n = .64$

$c_m = .31$

$c_{a_{ges}} = 0.60$

$c_n = .80$

$c_m = .36$

$\frac{p}{q}$

$c_{a_{ges}} = 0.70$

$c_n = .91$

$c_m = .38$

$\frac{p}{q}$

Wing chord, t

$c_{a_{ges}} = 1.27$

$c_n = 1.33$

$c_m = .33$

Wing chord, t
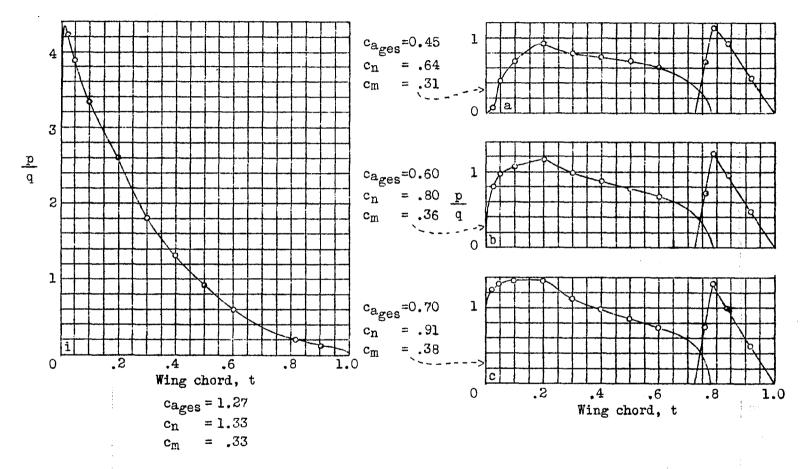
Figure 19i.- Pressure distribution for zero
setting of flap ($\beta = 0^{\circ}$).

Figure 20a to c.- Pressure distribution for a
flap deflection of $\beta = 19^{\circ}$.
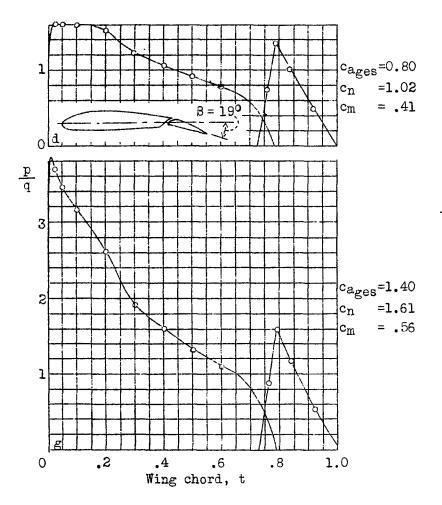
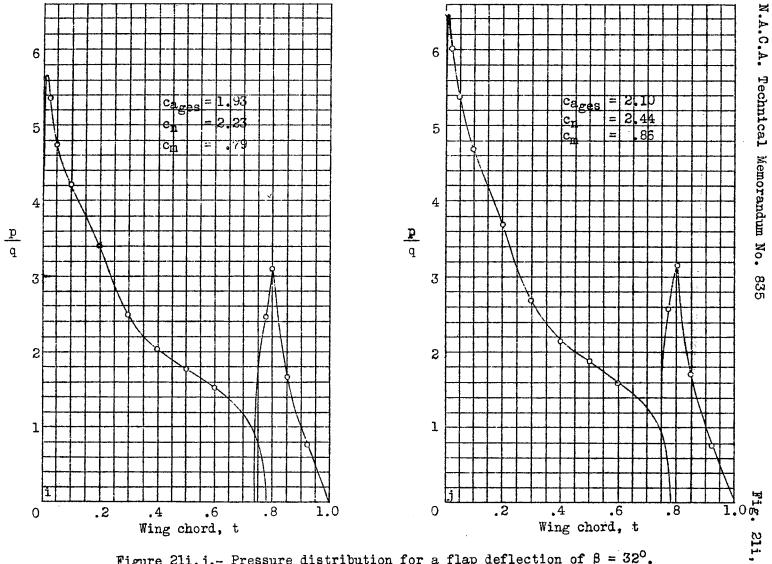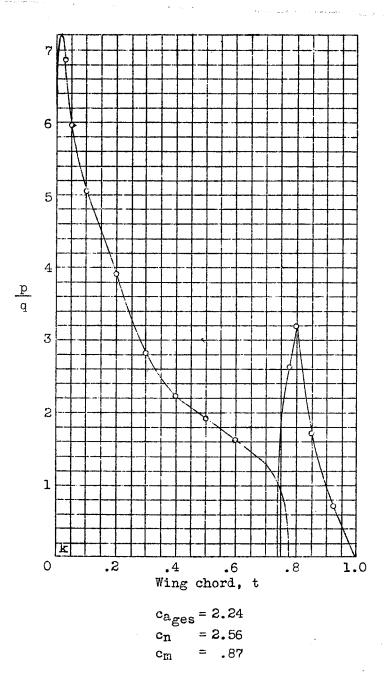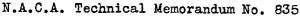Figure 20d to g.- Pressure distribution for a flap deflection of $\beta = 19°$.
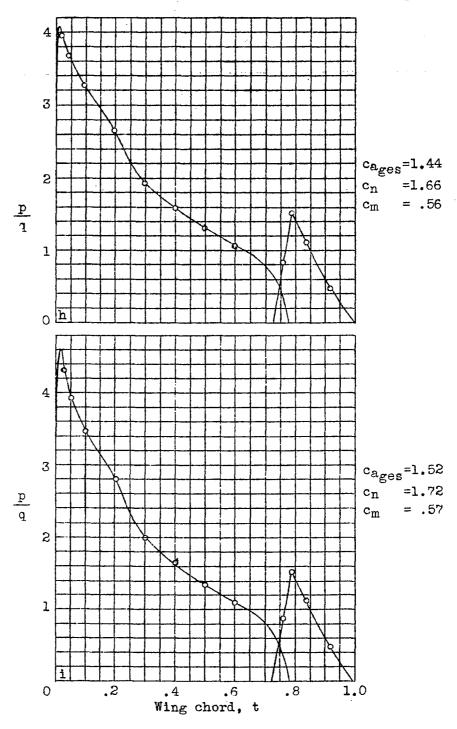
Figure 20h,i.- Pressure distribution for a flap deflection of $\beta = 19°$.

Figure 20j,k.- Pressure distribution for a flap deflection of β = 19°.

$\dfrac{p}{q}$

$\beta = 32°$

$c_{a_{ges}} = 0.70$
$c_n = .97$
$c_m = .48$

$c_{a_{ges}} = 0.80$
$c_n = 1.10$
$c_m = .51$

$c_{a_{ges}} = 1.00$
$c_n = 1.32$
$c_m = .56$

$c_{a_{ges}} = 1.20$
$c_n = 1.54$
$c_m = .63$

Wing chord, t

Wing chord, t
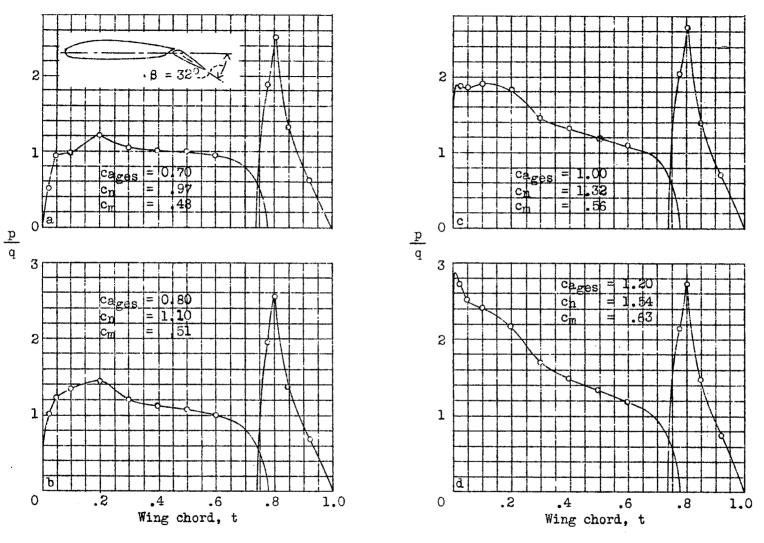
Figure 21a to d,- Pressure distribution for a flap deflection of $\beta = 32°$.
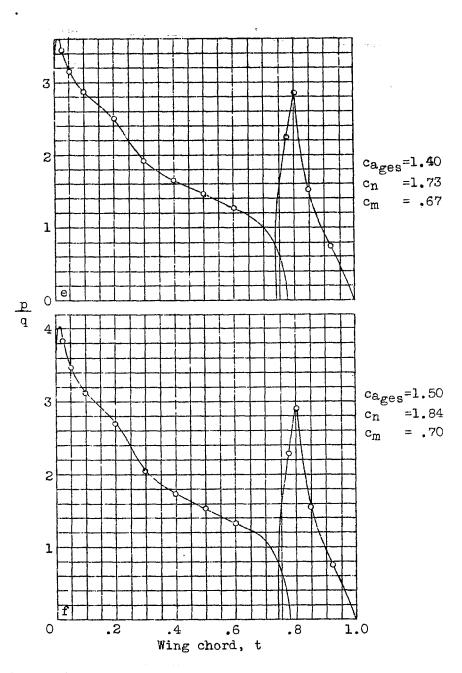
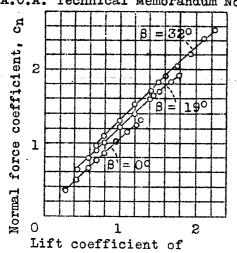Figure 21e,f.- Pressure distribution for a flap
deflection of β = 32°.
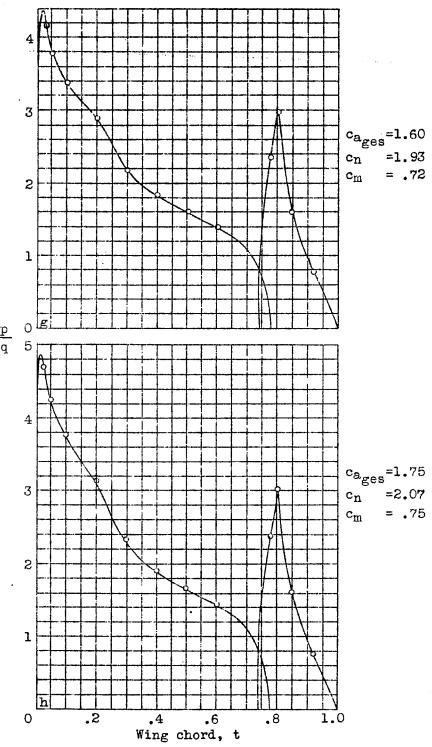
Figure 2lg,h.- Pressure distribution for a flap
deflection of β = 32°.

Figure 21i,j.- Pressure distribution for a flap deflection of ß = 32°.

$$c_{a_{ges}} = 2.24$$
$$c_n = 2.56$$
$$c_m = .87$$

Figure 21k.- Pressure distribution for a flap
deflection of $\beta = 32°$.

Figure 23.- Normal force coeffi-
　　　　　　cient c_n of the wing
section investigated as a func-
tion of the lift coefficient c_{ages}
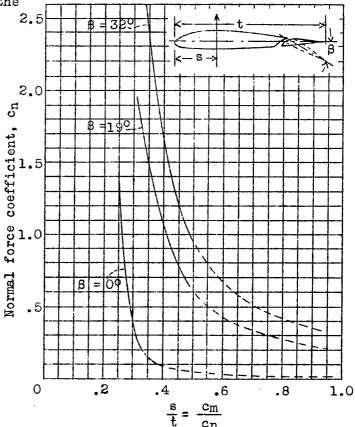of the complete airplane at the
several flap deflections.

$$\frac{dc_m}{d\beta} = 0.0068$$
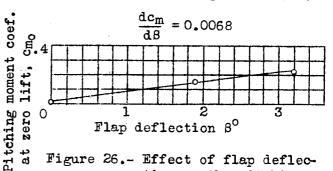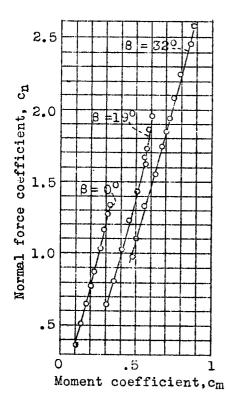
Figure 26.- Effect of flap deflec-
　　　　　　tion on the pitching
moment coefficient at $c_n = 0$

Figure 25.- Moment coefficient c_m
　　　　　　as function of the
normal force coefficient c_n for
various flap deflections β.

Figure 27.- Travel of center of
　　　　　　pressure as a function
of the normal force coefficient c_n.